~~SPECIFIED DISTRIBUTION ONLY~~

SC-DR-67-60

May 1967

MASTER

AERO-THERMODYNAMICS

Development Report

THE DEVELOPMENT OF EMPIRICAL EQUATIONS FOR PREDICTING DEPTH OF AN EARTH-PENETRATING PROJECTILE

C. W. Young, 9327

Sandia Laboratory, Albuquerque

SANDIA CORPORATION

PRIME CONTRACTOR TO THE U.S. ATOMIC ENERGY COMMISSION | ALBUQUERQUE, NEW MEXICO; LIVERMORE, CALIFORNIA; TONOPAH, NEVADA

~~SPECIFIED DISTRIBUTION ONLY~~

Issued by Sandia Corporation,
a prime contractor to the
United States Atomic Energy Commission

DISCLAIMER

DISCLAIMER

Portions of this document may be illegible in electronic image products. Images are produced from the best available original document.

AERO-THERMODYNAMICS

CFSTI PRICES

H.C. $ 3.00 ; MN. 65

SC-DR-67-60

THE DEVELOPMENT OF EMPIRICAL EQUATIONS FOR PREDICTING DEPTH OF AN EARTH-PENETRATING PROJECTILE

C. W. Young, 9327
Sandia Laboratory, Albuquerque

May 1967

ABSTRACT

An empirical equation is presented which allows a reasonably accurate prediction of the depth to which a projectile will penetrate the earth. Tables of soil constants and nose-performance coefficients are given for use in the equation.

TABLE OF CONTENTS

LIST OF ILLUSTRATIONS

LIST OF TABLES

LIST OF SYMBOLS

a	Unit of acceleration, 32.2 ft/sec^2
a_o, b_o, c_o, j	Constants
A	Frontal area of projectile, in.^{2}
C	Cohesion, KIPS/ft^2
CRH	Caliber radius head, for tangent ogive shapes
D	Total depth of penetration, measured along the path, ft
F	Force, lbs force
g	Acceleration due to gravity, ft/sec^2
IO	Inverse ogive nose shape
LL/PI	LL is liquid limit of a material, percent; PI is plasticity index of a material, percent
M	Mass, slugs
N	Constant, nose performance coefficient
"N"	Standard blow count, blows/ft
P	Total depth of penetration, measured along the path length, based on Poncelet and Petry equations, ft
S	Constant, dependent only upon soil properties
Sa/Si/Cl	Percentages of sand, silt, and clay that exist in a soil sample
S_d/S_s	Ratio of dynamic strength S_d of a soil to the static strength S_s of a similar soil sample. Both strengths are determined by triaxial compression tests.
TTR	Tonopah Test Range, Nevada
UNC	Unconfined compressive strength, KIPS/ft^2
V	Impact velocity, ft/sec
W	Weight of projectile, lbs
WC	Water content: ratio of weight of water to weight of solids, percent
WSMR	White Sands Missile Range, New Mexico
x_1	Cohesion strength of the soil, lbs/ft^2
x_2	Angle of internal friction, deg
x_3	Apparent soil viscosity

LIST OF SYMBOLS (Continued)

x_4	Soil density, lb/ft^3
x_5	Degree of saturation of the soil
Z	Position along a path length, ft
α	Air porosity; the ratio of volume of air to volume of constituents, percent
δ_t	Total density of the material, lb/ft^3
$\dot{\epsilon}$	Strain rate which is used in the dynamic strength tests, %/sec
ϕ	Angle of internal friction, deg

SUMMARY

An empirical equation is developed for prediction of total depth of penetration of a projectile in many earth targets. The equation development was based on approximately 200 full-scale penetration tests into a variety of targets, including rock, sandstone, gypsite, permafrost, ice, desert alluvium, silt, sand and saturated clay. Based on these tests, the error in depth prediction exceeds 20 percent in 9 percent of the tests, and 25 percent in less than 1.5 percent of the tests. The necessary tables of nose performance coefficients and soil constants are presented for more efficient engineering usage. The technique by which the depth of penetration into layered soils may be predicted is demonstrated, and a method by which the soil penetrability may be expressed in terms of soil properties is presented.

THE DEVELOPMENT OF EMPIRICAL EQUATIONS FOR PREDICTING DEPTH OF AN EARTH-PENETRATING PROJECTILE

Introduction

The problem of earth penetration by a projectile was studied as early as 1742. Since that time the most notable approaches have been taken by investigators Poncelet and Petry (References 1 and 2), although the empirical studies of each were generally concerned with the thickness of embankments required to protect personnel and facilities from artillery fire, and in each study the target was assumed to be a homogeneous natural earth target. The penetration depth-prediction equation developed by Petry in 1910 has been the most commonly used equation since that time.

In recent years, Sandia Laboratory has become increasingly interested in earth-penetration phenomena, and several reports on the development of penetration equations have been published (References 3, 4, and 5). However, the state of the art of earth penetration is still in its infancy, since the complicated problem has not been analytically solved.

A recent contribution to both a basic understanding of the mechanisms of earth penetration and a fundamental analytical approach to the problem was made by L. J. Thompson (Reference 6). However, it appears that a complete understanding of earth penetration is still some years in the future. In the meantime, empirically derived equations must be used to predict the penetration performance of vehicles or projectiles impacting the earth. In this report a penetration-prediction equation is presented which is intended to "bridge the gap" between the penetration-prediction equations of the Petry type and a much sought-after analytically determined equation based on a more complete understanding of earth penetration.

Historical Development

The starting point for each theory has been Newton's equation of motion

$$Mg - F = Ma_p, \tag{1}$$

which is a summation of the forces acting upon a projectile as it penetrates a target, where

M = mass of a projectile plus the soil moving with the projectile

g = acceleration due to gravity

F = soil resistance to movement

a_p = acceleration of projectile.

In general, the gravity force was neglected, and Equation (1) was rewritten as

$$-F = M_p V \frac{dV}{dZ}, \tag{2}$$

where V is the velocity of the projectile and Z is the distance the projectile travels within the target. Also, it was usually assumed that no soil moved with the projectile, and the mass of the projectile (M_p) only was considered.

Each investigator assumed the drag force, or soil resistance, to be of the general form

$$F = a_o + b_o V + c_o V^2, \tag{3}$$

where a_o, b_o, and c_o are constants. Some of the earlier investigators assumed that force was independent of velocity and depth, and proportional to the cross-sectional area of the projectile (i.e., the constants b_o and c_o were equal to zero). Poncelet assumed a slightly more complicated form of the drag function as

$$F = f_1(Z)\, f_2(V), \tag{4}$$

where

$$f_1(Z) = jA$$

and

$$f_2(V) = a_o + b_o V^2.$$

Again, a_o, b_o, and j are constants; therefore, Equation (4) is of the basic form of Equation (3). Substituting Equation (4) into Equation (2) and integrating gives the penetration equation

$$P = \frac{W}{2Ajb_o} \ell n \left(\frac{1 + b_o V^2}{a_o} \right), \tag{5}$$

where

P = total penetration distance, feet

W = weight of projectile, pounds

A = cross-sectional area of projectile, square inches

j, b_o, a_o = constants.

In general, most investigators since Poncelet have concentrated on evaluating the constants, a_o, b_o, and j. In 1910, Petry evaluated the constants and changed the form of the equation to

$$P = \frac{W}{A} K \log_{10}\left(1 + \frac{V^2}{215,000}\right), \tag{6}$$

where K is a constant which indicates the penetrability of the soils. Petry suggested a few values of K for some very general types of soil. The Petry equation is simple to use, and for several decades has been used with varying degrees of success.

Equation Development

Test Data

More than 200 full-scale earth-penetration tests were studied in the development of the empirical penetration equation presented herein. The details of these tests are given in Reference 7 through 11, plus several as yet unpublished reports by Sandia Laboratory. Table I lists some of the most pertinent test results which were used directly in the formulation of the equation.

For the purpose of this analysis, all targets are natural earth targets, impact is assumed at zero angle of attack, and penetration is approximately vertical. Earth penetration consists of a projectile: (1) impacting and entering the earth's surface, (2) moving through the soil, and (3) coming to rest in that soil. Neither a perforation, where a projectile travels completely through the target, nor tests into a man-made target are considered as natural earth-penetration tests. The only tests considered in the analysis and not included in Table I are those tests in which the depth of penetration was not sufficient for the mechanisms of earth penetration to come into play. The phenomenon of a projectile entering the earth's surface does not appear to be the same as that of a projectile moving through the earth. Although the mechanism of surface penetration is not well understood at this time, it appears that the depth of penetration must equal three vehicle body diameters plus the nose length before the surface effect is considered negligible in comparison to the soil penetration event.

General Form of the Equation

Rather than beginning with Newton's equation and attempting to develop semiempirically a drag function, as has been done in the past, development of the proposed equation begins with only an assumed form of the depth-prediction equation, including an assumption as to which parameters affect penetration. The equation is strictly empirical, but at this time sufficient high-quality penetration data are available to allow the development of such an equation with reasonable accuracy.

The total depth of penetration is assumed to be of the form:

$$D = f_1(N)\, f_2(A)\, f_3(W)\, f_4(V)\, f_5(S), \tag{7}$$

TABLE I

Test Data

Test No	Impact velocity (FPS)	Nose shape	W/A (psi)	Target*	Penetration Depth (ft)	Vehicle diameter (in.)	N**	S (average)
279-2	198	2.2 CRH	14.7	DL	5.7	4.4	0.82	5.6
279-3	111	6 CRH	14.7	DL	2.7	4.4	1.00	5.9
279-4	113	2.2 CRH	14.7	DL	2.0	4.4	0.82	5.3
279-5	168	2.2 CRH	14.7	DL	4.0	4.4	0.82	5.2
279-6	163	6 CRH	14.7	DL	4.6	4.4	1.00	5.2
279-7	110	9.25 CRH	14.7	DL	3.1	4.4	1.11	6.1
279-8	105	Flat	14.7	DL	1.3	4.4	0.56	5.6
279-9	172	Flat	14.7	DL	2.9	4.4	0.56	5.4
279-10	168	9.25 CRH	14.7	DL	5.3	4.4	1.11	5.1
279-12	166	2.2 CRH	14.7	DL	4.3	4.4	0.82	5.9
279-14	201	6 CRH	14.7	DL	6.5	4.4	1.00	5.3
279-16	175	2.2 CRH	10	DL	2.9	5.4	0.82	4.6
279-17	209	2.2 CRH	10	DL	4.2	5.4	0.82	4.9
279-18	172	9.25 CRH	10	DL	4.7	5.4	1.11	5.4
279-20	143	2.2 CRH	14.7	DL	3.3	5.4	0.82	5.7
279-21	165	2.2 CRH	14.7	DL	4.0	5.4	0.82	5.5
279-22	168	9.25 CRH	14.7	DL	6.0	5.4	1.11	5.9
279-23	138	9.25 CRH	14.7	DL	4.3	5.4	1.11	5.9
279-24	113	2.2 CRH	4.6	ST	2.7	8.0	0.82	-
279-25	112	2.2 CRH	10	ST	3.2	5.4	0.82	-
279-26	136	2.2 CRH	4.6	ST	3.3	8.0	0.82	-
279-27	173	2.2 CRH	10	ST	5.0	5.4	0.82	-
279-28	169	2.2 CRH	4.6	ST	4.6	8.0	0.82	-
279-29	116	9.25 CRH	10	ST	4.5	5.4	1.11	-
279-30	173	9.25 CRH	10	ST	6.4	5.4	1.11	-
279-31	204	2.2 CRH	4.6	ST	5.8	8.0	0.82	-
279-32	105	2.2 CRH	14.7	ST	2.6	4.4	0.82	-
279-33	214	9.25 CRH	10	ST	7.5	5.4	1.11	-
279-34	171	2.2 CRH	14.7	ST	5.5	4.4	0.82	-
279-35	110	2.2 CRH	14.7	ST	3.8	4.4	0.82	-
279-36	170	2.2 CRH	14.7	DL	4.0	4.4	0.82	5.3
279-37	105	Flat	14.7	DL	1.3	4.4	0.56	5.7
279-38	108	2.2 CRH	10	DL	2.0	5.4	0.82	6.9
279-39	139	9.25 CRH	20	DL	4.6	3.8	1.11	5.3
279-40	140	Flat	14.7	DL	1.8	4.4	0.56	4.8
279-41	172	2.2 CRH	14.7	DL	4.0	4.4	0.82	5.2
279-42	259	2.2 CRH	10	DL	6.5	5.4	0.82	5.1

TABLE I (Continued)

Test No.	Impact velocity (fps)	Nose shape	W/A (psi)	Target*	Penetration depth (ft)	Vehicle diameter (in.)	N**	S (average)
279-43	108	9.25 CRH	20	DL	2.9	3.8	1.11	5.3
279-44	167	Flat	14.7	DL	2.4	4.4	0.56	4.8
279-45	172	2.2 CRH	14.7	DL	3.9	4.4	0.82	5.0
279-46	170	2.2 CRH	14.7	DL	4.1	4.4	0.82	5.4
279-47	205	Flat	14.7	DL	2.9	4.4	0.56	4.2
279-49	210	9.25 CRH	10	DL	6.9	5.4	1.11	5.7
279-50	170	2.2 CRH	14.7	DL	4.1	4.4	0.82	5.4
279-51	112	9.25 CRH	29.2	DL	3.7	3.1	1.11	5.4
279-52	175	2.2 CRH	14.7	DL	4.3	4.4	0.82	5.4
279-53	132	Flat	14.7	DL	1.7	4.4	0.56	5.0
279-54	140	9.25 CRH	29.2	DL	5.1	3.1	1.11	5.2
279-55	213	2.2 CRH	14.7	DL	6.1	4.4	0.82	5.5
279-58	172	9.25 CRH	14.7	DL	5.1	4.4	1.11	4.9
279-59	171	2.2 CRH	5	DL	2.4	8.0	0.82	5.2
279-60	256	6.0 CRH	5	DL	5.4	8.0	1.0	4.8
279-61	349	6.0 CRH	5	DL	8.5	8.0	1.0	-
279-62	460	6.0 CRH	5	DL	9.5	8.0	1.0	-
279-63	502	6.0 CRH	5	DL	12.5	8.0	1.0	4.3
279-65	178	9.25 CRH	10	DL	4.5	5.4	1.11	4.9
279-66	180	9.25 CRH	10	DL	5.3	5.4	1.11	5.6
279-67	174	9.25 CRH	10	DL	4.7	5.4	1.11	5.3
279-68	178	9.25 CRH	10	DL	4.3	5.4	1.11	4.7
279-72	126	2.2 CRH	5	SC	13.8	8.0	0.82	50.0
279-80	158	9.25 CRH	5	ST	4.9	8.0	1.11	-
279-81	173	9.25 CRH	10	GY	2.3	5.4	1.11	2.6
279-83	274	9.25 CRH	10	GY	4.4	5.4	1.11	2.3
279-86	173	9.25 CRH	10	GY	2.9	5.4	1.11	3.3
279-88	255	9.25 CRH	10	GY	4.2	5.4	1.11	2.5
279-90	170	9.25 CRH	14.7	GY	3.1	4.4	1.11	3.0
314-2	163	Cone L/D = 2	5.3	DL	3.5	8.5	1.08	6.0
314-3	268	9.25 CRH	5.3	DL	5.9	8.5	1.11	4.2
314-4	265	Cone L/D = 2	5.3	DL	5.6	8.5	1.08	4.2
314-5	269	Cone L/D = 3	5.3	DL	7.1	8.5	1.32	4.3
314-7	167	Cone L/D = 3	5.3	DL	4.1	8.5	1.32	5.5
314-9	158	Conic step	5.3	DL	3.9	8.5	1.28	5.9
314-10	254	Conic step	5.3	DL	6.4	8.5	1.28	4.4
314-11	259	Biconic	5.3	DL	6.8	8.5	1.31	4.4
314-12	161	Biconic	5.3	DL	4.1	8.5	1.31	5.9

TABLE I (Continued)

Test No.	Impact velocity (fps)	Nose shape	W/A (psi)	Target*	Penetration depth (ft)	Vehicle diameter (in.)	N**	S (average)
314-13	269	Short IO	5.3	DL	5.5	8.5	1.03	4.3
314-15	162	IO	5.3	DL	4.3	8.5	1.32	6.1
314-16	260	IO	5.3	DL	6.7	8.5	1.32	4.3
314-17	195	IO	5.3	DL	4.8	8.5	1.32	5.0
314-18	195	Cone L/D = 3	5.3	DL	5.1	8.5	1.32	5.3
314-19	315	Cone L/D = 3	5.3	DL	8.8	8.5	1.32	4.2
314-20	220	Cone L/D = 3	7.1	DL	7.8	8.5	1.32	5.7
314-21	195	Cone L/D = 3	8.0	DL	6.3	8.5	1.32	5.3
314-22	196	IO	8.0	DL	6.2	8.5	1.32	5.2
314-23	236	IO	7.1	DL	7.3	8.5	1.32	4.8
314-27	307	IO	5.3	GY	4.3	8.5	1.32	2.1
314-28	350	Cone L/D = 3	5.3	GY	4.7	8.5	1.32	1.9
314-30	265	Cone L/D = 3	5.3	GY	3.6	8.5	1.32	2.2
314-32	262	IO	5.3	GY	3.7	8.5	1.32	2.3
314-36	350	IO	5.3	GY	5.0	8.5	1.32	2.0
314-37	(265)	IO	5.3	DL	6.9	8.5	1.32	4.3
314-39	(265)	Cone L/D = 3	5.3	DL	7.2	8.5	1.32	4.5
314-45	258	IO	5.3	GY	4.0	8.5	1.32	2.6
314-46	257	Cone L/D = 3	5.3	GY	3.8	8.5	1.32	2.5
7R	984	9.25 CRH	15.3	DL	52.5	9.0	1.11	-
122-1	252	12.5 CRH	22.5	DL	13.0	18.0	1.22	-
122-2	901	12.5 CRH	27.6	DL	65.0	18.0	1.22	-
124-1	305	6.0 CRH	20.0	DL	12.8	9.0	1.0	-
124-2	492	6.0 CRH	19.9	DL	17.0	9.0	1.0	-
124-3	713	6.0 CRH	19.9	DL	38.0	9.0	1.0	-
124-4	394	6.0 CRH	19.9	DL	16.6	9.0	1.0	-
124-5	780	6.0 CRH	19.3	P	34.5	9.0	1.0	3.8
124-6	400	6.0 CRH	19.5	P	15.5	9.0	1.0	3.8
124-7	400	6.0 CRH	20.0	P	15.0	9.0	1.0	3.7
124-8	580	6.0 CRH	19.5	P	25.5	9.0	1.0	3.9
124-9	427	6.0 CRH	20.1	SA	25.8	9.0	1.0	5.7
124-10	401	6.0 CRH	19.5	SA	34.5	9.0	1.0	8.2
124-11	684	6.0 CRH	19.5	SA	50.5	9.0	1.0	6.3
124-12	641	6.0 CRH	20.1	SA	50.5	9.0	1.0	5.9
124-15	330	9.25 CRH	8.1	DL	11.5	8.0	1.11	-
124-16	520	9.25 CRH	8.1	DL	13.6	8.0	1.11	-
124-17	669	9.25 CRH	8.1	DL	18.5	8.0	1.11	-
124-18	562	9.25 CRH	10.7	DL	18.2	8.0	1.11	-
124-19	570	9.25 CRH	11.8	DL	17.7	8.0	1.11	-
124-20	558	9.25 CRH	10.1	DL	16.5	8.0	1.11	-

TABLE I (Continued)

Test No.	Impact velocity (fps)	Nose shape	W/A (psi)	Target*	Penetration depth (ft)	Vehicle diameter (in.)	N**	S (average)
124-21	565	9.25 CRH	11.8	DL	18.7	8.0	1.11	-
124-22	387	9.25 CRH	10.1	DL	13.0	8.0	1.11	-
124-23	385	9.25 CRH	11.8	DL	12.7	8.0	1.11	-
124-24	380	9.25 CRH	10.1	DL	12.8	8.0	1.11	-
124-26	750	9.25 CRH	11.9	DL	20.0	8.0	1.11	-
124-27	514	9.25 CRH	8.1	DL	17.2	8.0	1.11	-
124-30	(78)	9.25 CRH	17.3	M	16	9.0	1.11	40.
120-6	256	2.2 CRH	16.0	DL	9.2	9.0	0.82	-
120-7	447	2.2 CRH	15.6	DL	14.1	9.0	0.82	-
120-9	458	6.0 CRH	14.2	DL	14.2	9.0	1.00	-
120-10	243	9.25 CRH	14.9	DL	10.2	9.0	1.11	-
120-14	681	9.25 CRH	17.4	DL	24.4	9.0	1.11	-
120-15	467	6.0 CRH	14.2	DL	13.8	9.0	1.0	-
120-23	480	6.0 CRH	14.0	I	18.0	9.0	1.0	4.1
120-24	480	6.0 CRH	14.0	I	18.5	9.0	1.0	4.2
120-56	723	Flat	19.8	DL	19.0	9.0	0.56	-
120-57	548	Flat	19.5	DL	13.6	9.0	0.56	-
120-70	297	Flat	20.4	DL	7.75	9.0	0.56	-
120-83	590	Flat	16.5	DL	17.0	9.0	0.56	5.0
120-89	600	Flat	10.0	DL	13.1	9.0	0.56	4.8
120-97	650	Flat	16.5	DL	15.3	9.0	0.56	4.1
3A	1050	2.2 CRH	16.4	DL	55.4	9.0	0.82	-
4A	1052	2.2 CRH	16.5	SA	70.0	9.0	0.82	7.4
5A	1077	9.25 CRH	18.2	DL	73.0	9.0	1.11	-
6A	1060	2.2 CRH	16.4	DL	52.5	9.0	0.82	-
8A	906	9.25 CRH	18.1	DL	57.0	9.0	1.11	-
120-5	877	9.25 CRH	18.1	SA	71.0	9.0	1.11	6.3
120-26	955	6 CRH	17	SA	63.3	9.0	1.0	5.9
120-42	959	6 CRH	14	DL	53.5	9.0	1.0	-
120-77	1065	9.25 CRH	13.3	R	13.0	9.0	1.1	1.07
120-60	1037	6 CRH	16.1	DL	53.5	9.0	1.0	-
120-103	(880)	9.25 CRH	12.2	SS	10.0	8.	1.1	1.3
120-112	(820)	9.25 CRH	14.3	SS	10.2	10.188	1.1	1.3
1R	1030	2.2+ CRH Flat	16.5	DA	38.	9.	0.8	4.1
2R	1020	2.2+ CRH Flat	16.3	DA	37.6	9.	0.8	4.1
4R	976	2.2 CRH	16.0	DA	36.2	9.	0.82	4.1
5R	955	2.2 CRH	16.9	DA	45	9.	0.82	5.0

*See Table III for nomenclature and description.

**See Table II.

where

D = depth of penetration, measured along the penetration path, feet

V = velocity, feet per second

S = either a constant, dependent only upon soil properties averaged over the depth of penetration, or a function, based upon fundamental soil properties

W = total vehicle weight, pounds

A = cross-sectional, or frontal area, square inches

N = constant, vehicle nose-performance coefficient.

It is realized that Equation (7) is not the most general form of the solution. Indeed, if the actual solution to the problem is assumed to be represented by a generalized Taylor series expansion in six-dimensional space, then Equation (7) is only one term of the most general solution. By assuming the form of Equation (7), it is implied that the constant in each of the other terms of the general solution is equal to zero. However, the form of Equation (7) was assumed because:

1. It is simple, thus lending itself to a development based primarily upon engineering judgment.
2. It is similar in form to previously developed equations which showed some degree of reliability.
3. The crucial assumption that all other constants of the general solution are approximately zero may readily be verified by the closeness of the final data fit.

In Equation (7) it is assumed that all test and vehicle parameters are included in the first four functions, and that all the soil properties are included in the fifth function. (Because some soil properties are rate-dependent, this is perhaps an oversimplification of the problem.) Two additional vehicle parameters should be mentioned:

1. The probe diameter is important but is, in effect, included in the area. However, since this equation is not intended to encompass any scaling laws, it should be noted that to be termed a full-scale test the vehicle diameter should be at least 3 inches. The largest vehicle diameter used in the tests on which this analysis is made was 18 inches, and no significant scaling problems were noted in the 3-inch to 18-inch diameter range.
2. The second vehicle parameter to consider is the total length. As yet, no experimental test program has been conducted to determine the effect of fineness ratio (length of vehicle divided by diameter) on depth of penetration, but it appears that a minimum fineness ratio of 10 is necessary to assure stability during penetration. Also, a fineness ratio of greater than 20 should be avoided because of the increased side-wall friction during penetration.

Development of Individual Functions

The general approach to solving Equation (7) is to hold four of the functions constant and solve for the fifth. To follow the general approach strictly would involve a formidable number of tests, so the actual approach to solving the equation is one of experimental iteration. If sufficient test data are not available to solve for one function with the other four functions held constant, then additional test data are "normalized" to a standard set of conditions before they are used. The equation used to normalize the data is the "best" empirical equation available at that stage of the analysis. The more accurate the equation becomes in subsequent iterations, the more nearly exact become the normalized data, and in the limit each function becomes an exact fit to the real data. Appendix A gives an example of the iterative technique used in normalizing the data.

In the following paragraphs, each of the five functions is developed and discussed. However, only the final iteration and the final form of the function are given.

Nose Shape Effect, $f_1(N)$ -- The first function to be developed is that for the nose-shape effect, since more data are available with each of the other four functions held constant. Figure 1 is a plot of the data from which $f_1(N)$ is determined. For the target used, the soil is homogeneous, both laterally and vertically. Therefore, for one set of test conditions (V, W/A, and soil), assuming no nose-shape effects, the depth of penetration should always be constant. Any deviation from a constant depth when various nose shapes are used is an indication of nose performance. The nose-shape effect, $f_1(N)$, is best described by a nose-performance coefficient, rather than by an actual function. Based on the curve drawn in Figure 1, the final nose-performance coefficients are determined to be:

Flat nose,	N = 0.56
2.2 CRH,	N = 0.82
6.0 CRH,	N = 1.00 (arbitrarily chosen as the standard)
9.25 CRH,	N = 1.11

The performance coefficients determined from Figure 1 are for tangent ogive nose shapes, and for the flat nose. Most of the tests considered were conducted using one of the above nose shapes, and therefore the remainder of the equation development is based on the above coefficients.

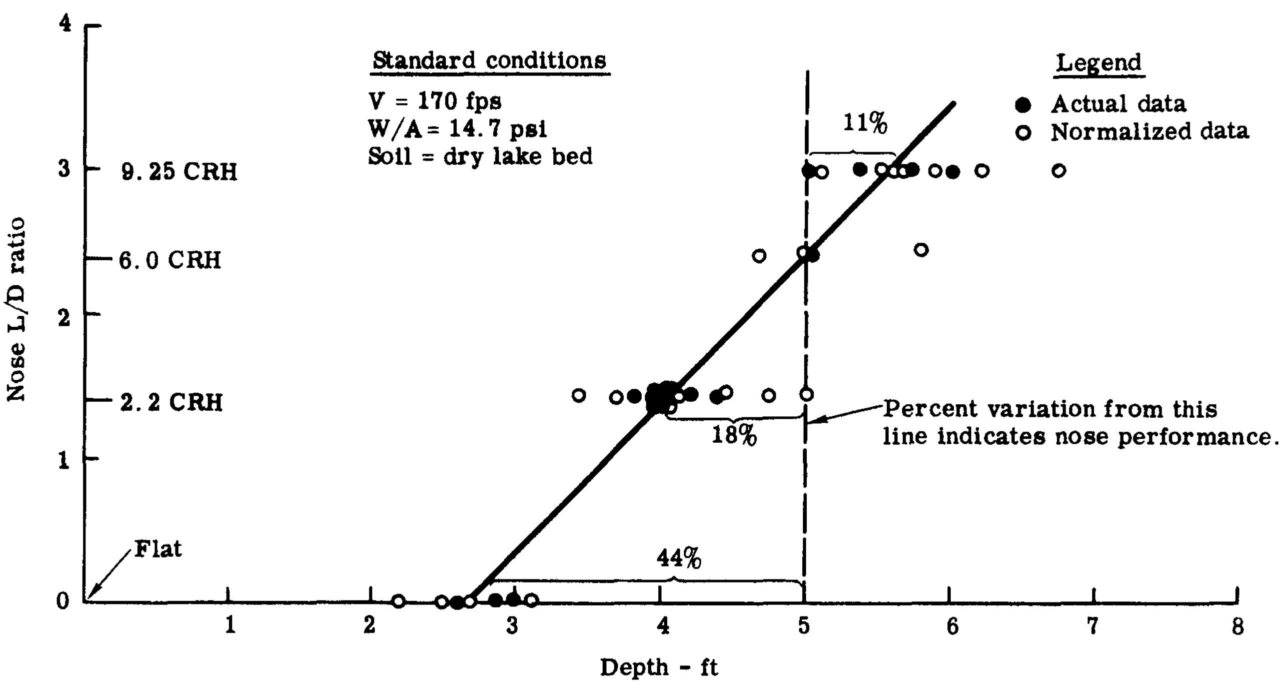

Figure 1. Nose-Shape Effect

Additional nose-performance coefficients are determined from a series of tests during which all parameters were held constant except nose shape. Any variation in penetration performance (an average of several tests) was then attributed to the nose performance, again using the 60.0 CRH tangent ogive as the standard, and nose-performance coefficients were calculated. These coefficients are presented in Table II.

TABLE II

Nose-Performance Coefficients
(Based on 6.0 CRH Tangent Ogive as 1.0)

Nose shape	Coefficient
Flat nose	0.56
2.2 CRH tangent ogive	0.82
6.0 CRH tangent ogive	1.00
9.25 tangent ogive	1.11
12.5 CRH tangent ogive	1.22
Cone, $\ell/d^{*} = 2$	1.08
Cone, $\ell/d = 3$	1.32
Conic step, cone plus cylinder plus cone	1.28
Biconic, $\ell/d = 3$	1.31
Short inverse ogive, $\ell/d = 2$	1.03
Inverse ogive, $\ell/d = 3$	1.32

* ℓ/d is the ratio of the nose length to major diameter.

Weight and Area Effect, $f_2(A)$ and $f_3(W)$ -- The No. 279 series of tests was conducted under closely controlled conditions, including very similar soil conditions. It appears that sufficient data are available to justify combining $f_2(A)$ and $f_3(W)$ into a single function, $f_6\left(\frac{W}{A}\right)$. Figure 2 is a plot of impact velocity versus depth of penetration with all test conditions held constant, except that the vehicle weight and area are varied in the same ratio. It appears that the use of $f_6(W/A)$ is reasonable.

W/A Effect, $f_6(W/A)$ -- Figure 3 shows the effect of W/A on depth. Each data point is a composite or average of all tests meeting those conditions of W/A and velocity. With W/A plotted against depth, the slope on a log-log plot is approximately 1/2; therefore, it appears that $f_6(W/A) = (W/A)^{1/2}$ best describes the effect of W/A on depth of penetration. The curves of Figure 3 demonstrate the fit of the test data to the empirically determined function for $f_6(W/A)$.

The development of $(W/A)^{1/2}$ represents a significant deviation from the theories postulated in all previous analyses of earth penetration, such as the Petry and Poncelet formulations in which $(W/A)^1$ was used.

The effect of weight and area is:

$$f_6(W/A) = (W/A)^{1/2}$$
$$f_2(A) = (1/A)^{1/2} = (A)^{-1/2}$$
$$f_3(W) = (W)^{1/2}$$

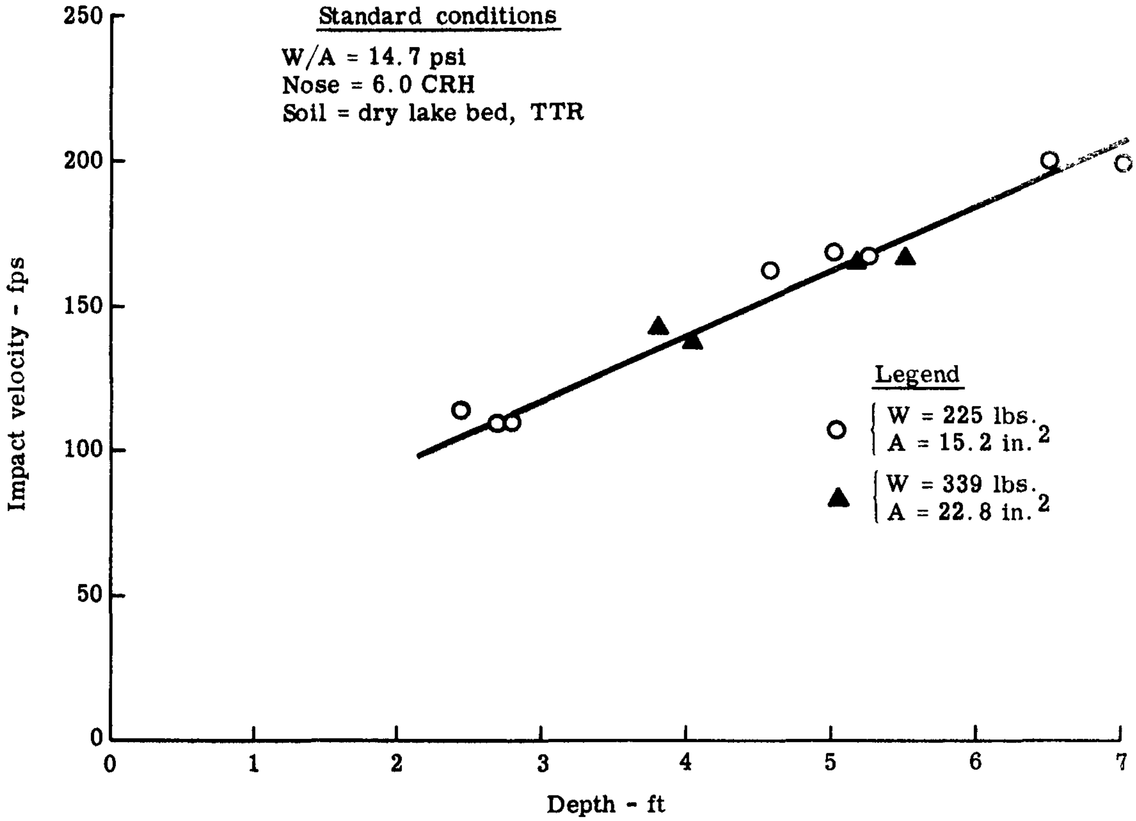

Figure 2. Effect of Varying Weight and Area in Same Ratio

The Velocity Effect, $f_4(V)$ -- Since most soils considered in this analysis are vertically homogeneous for only the top few feet, it is not practical to hold the soil function constant over the complete range of velocities. The approach is to determine the velocity effect for the low velocity ran; , during which the soil function may be assumed constant, and then separately determine the velocity effect for the high velocity range.

Figure 4 shows a plot of velocity versus depth over the low velocity range. The curve to best fit the data appears to be $f_4(V) = C_1 \ell n\,(1 + 2V^2 10^{-5})$, for an impact velocity of less than 200 feet per second. A break in the curve appears at about 200 feet per second, above which a second function of velocity must be used. The constant, C_1, is completely arbitrary.

It is well known that the Main Dry Lake at TTR is a layered material. Thus far in the analysis, only the top 10 feet of the lake have been considered. To determine the high velocity effect, a preliminary set of soil constants was calculated and used to normalize the data to that used in the low velocity part of the velocity effect function. Figure 5 shows the normalized and actual data and the curve representing the best data fit. The high velocity function appears to be $C_2(V - 100)$. The constant, C_2, must be determined such that at an impact velocity of 200 feet per second (the break between the low and high velocity ranges), the low and high velocity functions are equal.

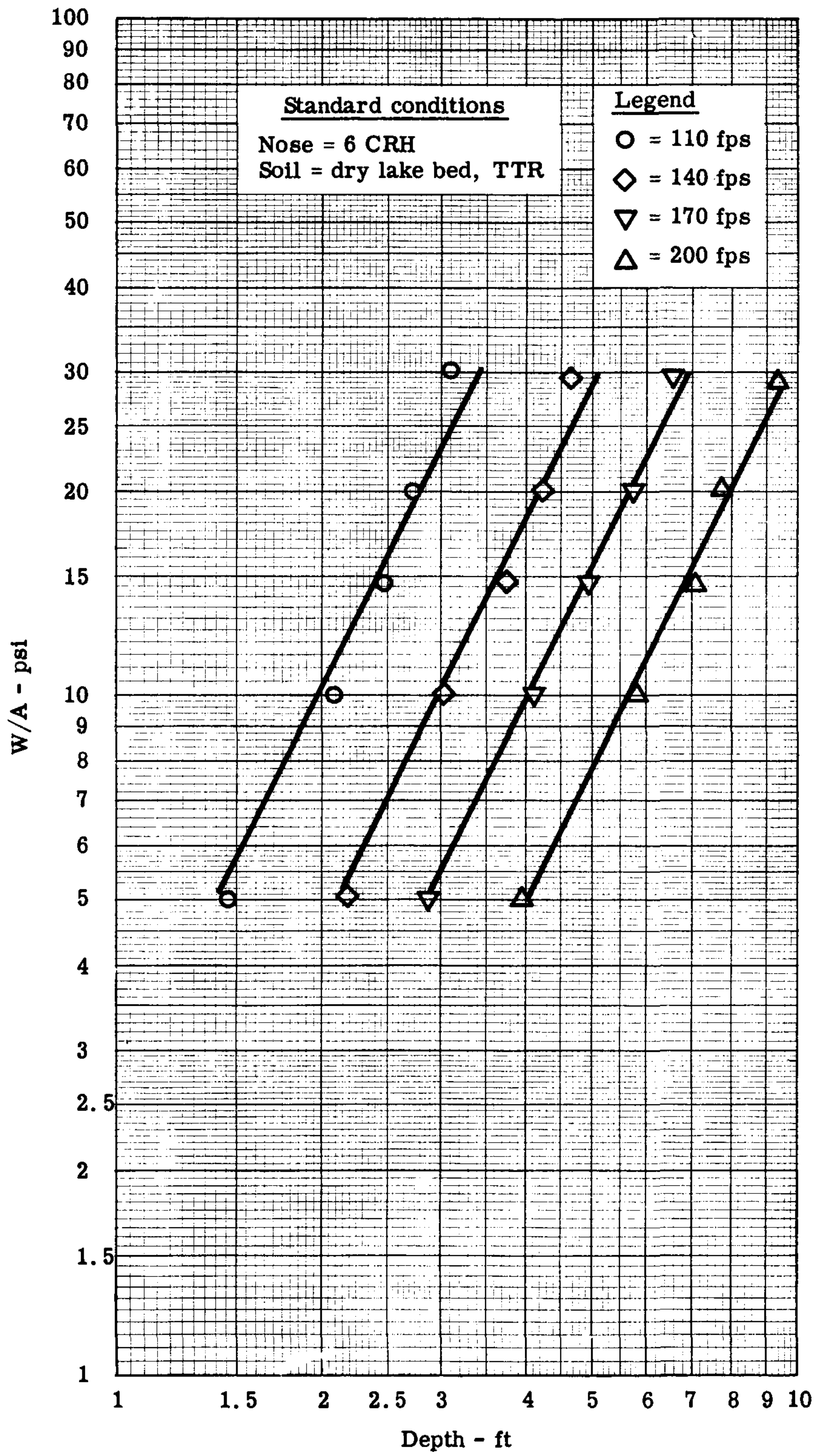

Figure 3. W/A Effect on Depth of Penetration

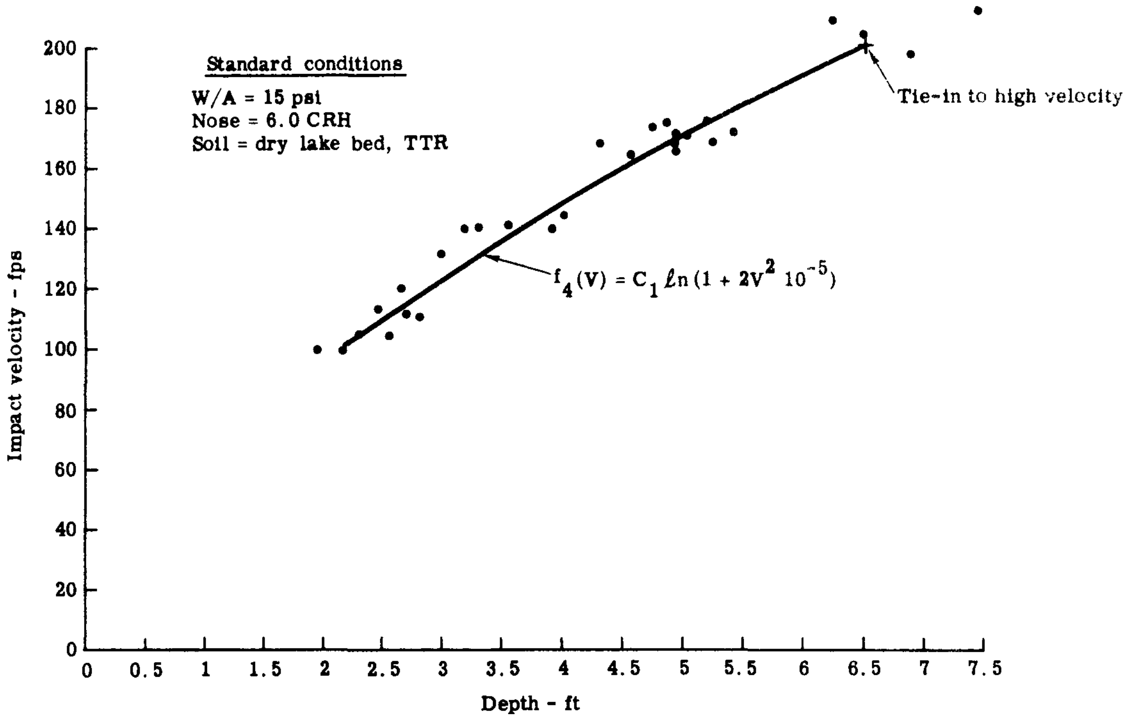

Figure 4. Low Velocity Effect

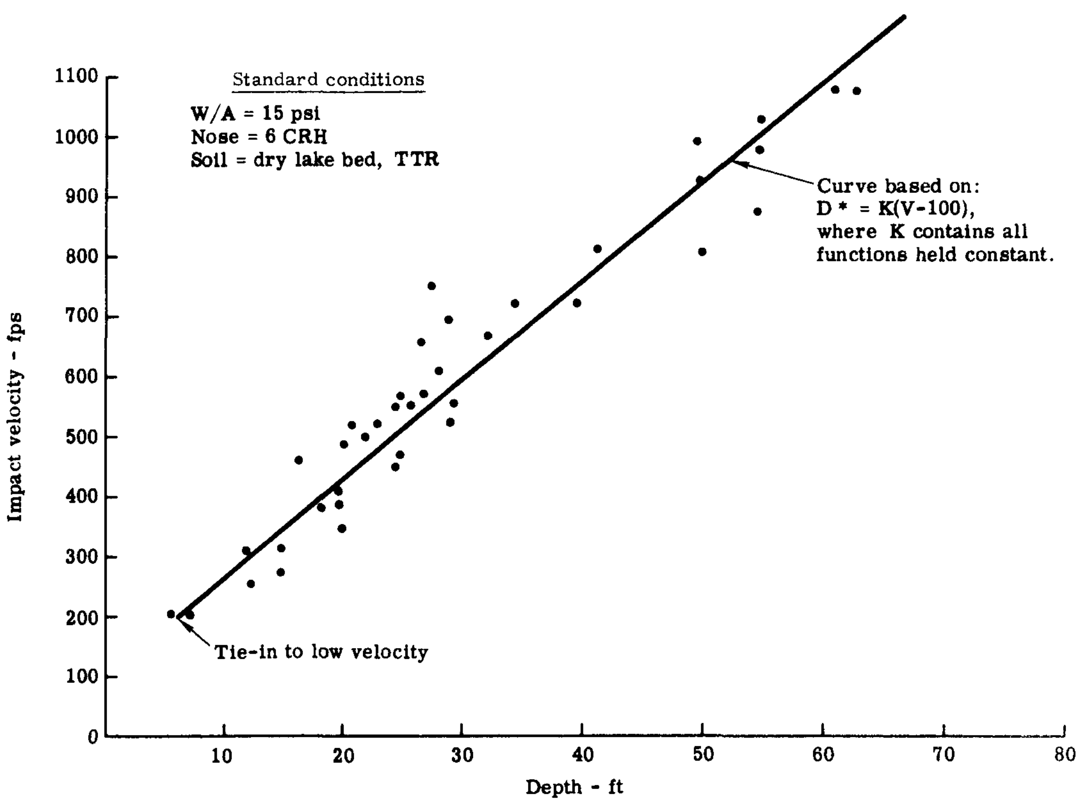

Figure 5. High Velocity Effect

The velocity effect function, $f_4(V)$ is:

$$f_4(V) = C_1 \ln(1 + 2V^2 10^{-5}), \qquad V < 200 \text{ feet per second},$$

$$f_4(V) = C_2 (V - 100), \qquad V \geq 200 \text{ feet per second}.$$

The Effect of Soils, $f_5(S)$ -- It is recognized that $f_5(S)$ is a complicated function relating the various soil properties to some "index of penetrability." Insufficient data are available at this time for the full development of the function, but the technique for that development is presented in Appendix B.

After a penetration is conducted at a site, a soil constant, S, may be determined based on the equation developed in this report. Such a soil constant is an average, based on the entire path of penetration. Table III is a listing of the targets considered in this analysis, with a very general description of each, and the average soil constant for each type of soil or target. The single average soil constant is quite adequate for homogeneous soil, but for layered soils, such as the Main Dry Lake at TTR, it is necessary to use different soil constants for each layer, as explained in Appendix C.

Soil constants may be obtained in any of three methods:

1. If a previous test has been conducted in the immediate area, then a soil constant may be calculated from that test, and that constant may then be used for future depth predictions in the same area.
2. A soil constant may be estimated if the soil properties and geology of the proposed test area are studied and compared to a similar area where a soil constant is already known. For example, the soil condition of the top few feet at Antelope (Ben's) Dry Lake at TTR is similar to that of the Main Dry Lake at TTR; therefore, the same soil constant could be used for the first depth prediction at Antelope Dry Lake.
3. A soil constant could be calculated, by the method outlined in Appendix B, provided adequate dynamic soil properties could be obtained.

At present, it is necessary to depend most heavily on methods 1 and 2, but it is hoped that, in the near future, method 3, outlined earlier, may be used.

The Penetration Equation

In summary, the functions developed thus far are:

$$f_1(N) = (\text{Nose-Performance Coefficients, Table II})$$

$$f_2(A) = (A)^{-\frac{1}{2}}$$

TABLE III

Target Nomenclature and Soil Constants

Code	Site	Description	Depth (ft)	Mechanical Properties "N" (BLS/ft)	UNC (KIPS/ft^2)	ϕ (deg)	C (KSF)	S_d/S_s	$\dot{\epsilon}$ (%/sec)	δ_t lb/ft^3	WC (%)	α (%)	LL/PI (%)	Sa/Si/Cl (%)	Soil constant S
DL	TTR, Main Dry Lake	Clayey silt, silty clay, dense, hard	0-8	60	16.0	-	-	-	-	107	15	21	38/9	2/18/79	5.2
		Sand, silty, very dense, dry, cemented	8-25	180	16.0	-	-	-	-	116	10	25	39/8	70/15/15	2.5
		Sand, silty, clayey, very dense	25$^+$	61	10.0	-	-	-	-	117	13	17	29/8	70/20/10	5.2
ST	Salt, Target WSMR	Clay, silty, soft, wet, brown	0-1.6	-	0.5	-	-	-	-	110	37	4	-	11/22/67	40
			1.6$^+$	20	4.0	42	0.9	2.4	4.5	130	25	0	-	23/44/33	6.5
SC	Great Salt Lake Desert, Utah	Clay, soft, wet, grey, varved, medium to high plasticity	0-15$^+$	-	0.6	25	0.2	1.7	-	105	71	0	52/17	0/50/50	50
GY	Northrup Strip, WSMR	Gypsite, selenite, hard, moist, very homogeneous	0-10$^+$	-	11.0	38	4.1	2.0	-	122	37	0	-	-	2.5
I	Gulkana Glacier Alaska	Ice, glacier	0-20$^+$	-	-	-	-	-	-	-	-	-	-	-	4.15
P	Eielson AFB, Alaska	Silt, clayey, frozen, (Permafrost)	0-30$^+$	-	-	-	-	-	-	-	-	-	-	-	3.8
SA	Eglin AFB Florida	Sand, loose, moist	0-70$^+$	16	-	-	-	-	-	114	7	25	-	95/-/5	6.5
R	NTS, TTR, Nevada	Rock, highly welded, fine-grained agglomerate	0-10$^+$	-	-	-	-	-	-	-	-	-	-	-	1.0[illegible]
SS	Grants, N.M.	Sandstone	0-30$^+$	-	-	-	-	-	-	-	-	-	-		
M	Skaggs Island California	Clay, silty, wet (bay mud)	0-50$^+$	-	[illegible].2	-	-	-	-	10[illegible]	75	[illegible]	72/[illegible]	[illegible]/70	[illegible]
DA	TTR, Nevada	Sand, silty, clayey, dense (desert alluvium)	0-100$^+$	-	-	-	-	-			-	-			[illegible]

$f_3(W) = (W)^{\frac{1}{3}}$

$f_4(V) = C_1 \ln(1 + 2V^2 10^{-5})$, $\quad V < 200$ feet per second

$f_4(V) = C_2(V - 100)$, $\quad V \geq 200$ feet per second

$f_5(S)$ = Soil constant, or function.

The ratio between C_1 and C_2 must be adjusted so that the velocity terms are equal at 200 feet per second, but the value of either constant is arbitrary. If the value of C_1 is chosen to be 0.53, then C_2 is determined to be 0.0031. The final form of the equation is:

$$D = 0.53SN(W/A)^{\frac{1}{3}} \ln(1 + 2V^2 10^{-5}), \quad V < 200 \text{ feet per second} \tag{8}$$

$$D = 0.0031SN(W/A)^{\frac{1}{3}}(V - 100), \quad V \geq 200 \text{ feet per second.} \tag{9}$$

A preliminary check on the validity of an equation is to test the effect of varying the parameters on some known quality other than the one being calculated. In this case, the total depth is being calculated, but also the acceleration signature from most tests is available (References 7 through 10) and may be used as an experimental check. From elementary energy concept,

$$FD = \frac{1}{2} MV^2. \tag{10}$$

If, in Newton's equation of motion,

$$Mg - F = ma_p \tag{1}$$

the gravitational force is neglected, it is possible to combine Equations (10) and (1) to obtain

$$Ma_p = \frac{mV^2}{2D}. \tag{11}$$

Equation (9), for example, may then be used in Equation (11) to obtain

$$a_p = \frac{V^2}{2(0.0031)SN\sqrt{W/A}(V - 100)}. \tag{12}$$

From Equation (12), the following general observations may be made:

1. As the impact velocity is increased, the average deceleration increases.
2. As the vehicle weight is increased the average deceleration decreases.
3. For large soil constants (corresponding to soft soil), the average deceleration is small.
4. The more-pointed noses provide lower average decelerations.
5. Increasing the area results in an increased average acceleration.

References 7 through 10 show that each of the observations pertaining to Equation (12) is verified by experimental data.

Figures 6 and 7 are nomograms based on Equations (8) and (9), and are in general easier to use than equations. As an example of the use of the nomograms, assume an 8-inch-diameter vehicle, weighing 300 pounds, and with a 9.25 CRH nose; the desired impact velocity is 400 fps, and the target is a dry lake playa of clayey silt. From Table II the nose performance coefficient, N, is found to be 1.11; and from Table III the soil constant, S, is found to be 5.2. For the low velocity range the nomogram in Figure 6 provides the greater accuracy. Beginning with the "vehicle diameter" of 8 inches, on the lower left vertical axis, and following the dashed line as shown on Figure 6, the predicted depth of penetration is determined to be 12.7 feet.

The development of the equation is based primarily upon obtaining an empirical equation which adequately fits the test data. Therefore, the questions are: "How well does the equation fit the data?" and "Is the proposed equation significantly better than the currently used equation?" Figure 8 shows a fit of the TTR Main Dry Lake test data to a curve representing the Petry equation. Figure 9 is a similar plot showing the data fit to the curve described by the proposed penetration depth prediction equation. The data plotted on Figure 9 were taken from the tests conducted at the TTR Main Dry Lake, and also from all tests listed in Table I and targets described in Table III. Based on these tests, the error in depth prediction exceeds 20 percent in 9 percent of the tests, and 25 percent in less than 1.5 percent of the tests.

The data scatter in Figure 9 is well within the expected soil homogeneity of any natural earth target. Also, part of the data scatter is the result of errors in the data itself; for example, the velocity may be in error by ±5 percent, which would in turn induce a 3-percent error in the data fit.

Recommendations for Future Work

Since by far the least well-defined term in the depth prediction equation is the soil constant, or soil function, it is only natural that future work will be concerned primarily with the soil itself.

Additional field tests must be conducted to determine the penetration resistance of several soils not yet investigated. The listing in Table III may then be extended, and, with the broader foundation of experimental results from which to work, it will be possible to estimate better a soil constant for any desired test site. During future field tests more emphasis must be placed on obtaining complete soil properties at each impact site, and on making detailed observations of the effect on the soil as a result of the penetration event.

The other area in which considerable effort must be expended is that of obtaining an expression to describe the soil function, or soil constant, in terms of the soil properties. An effort is already under way to develop equipment to obtain dynamic soil properties, and, as these soil properties become available, the soil function may then be improved upon.

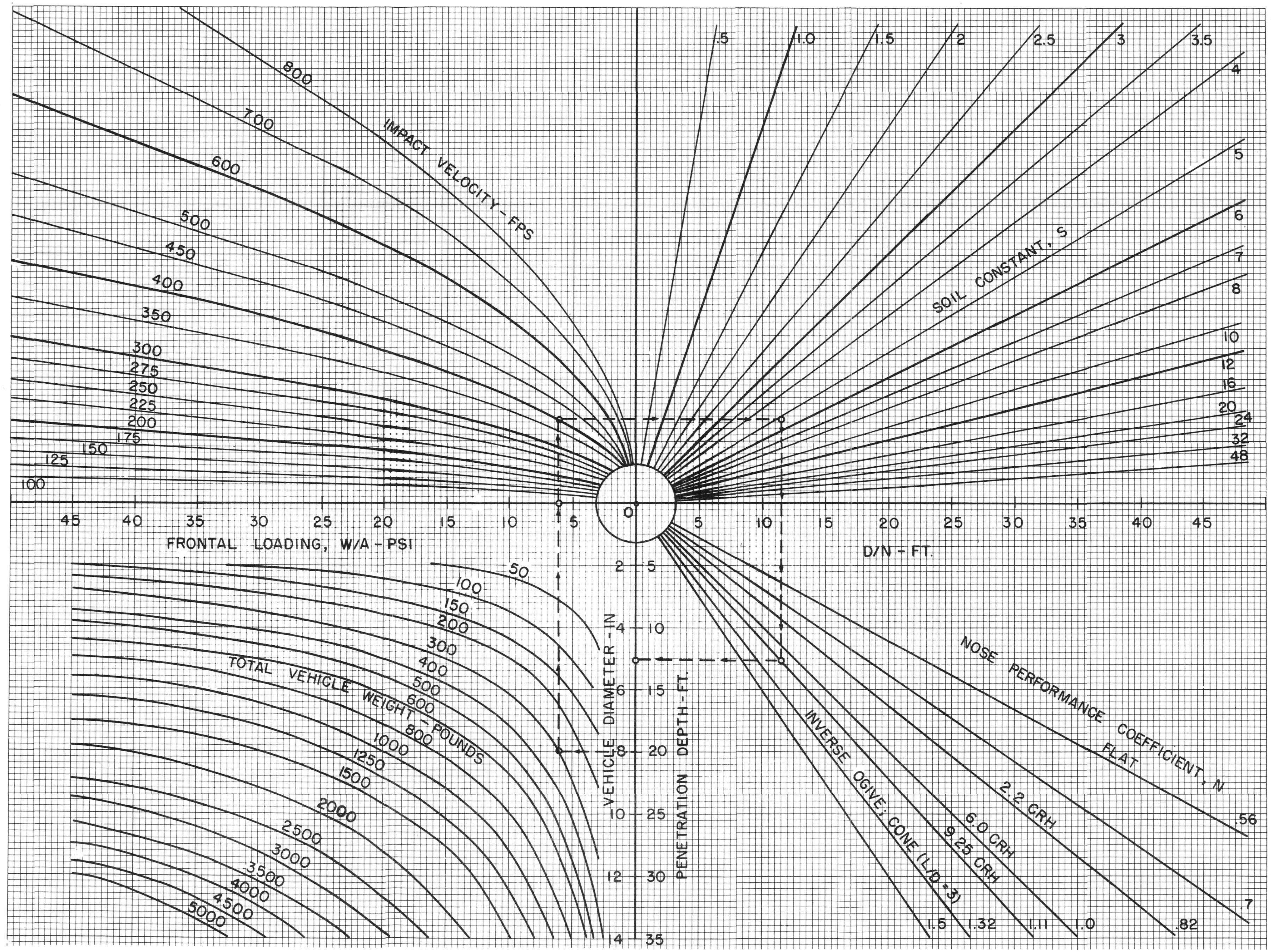

Figure 6. Low-Velocity-Penetration Nomogram

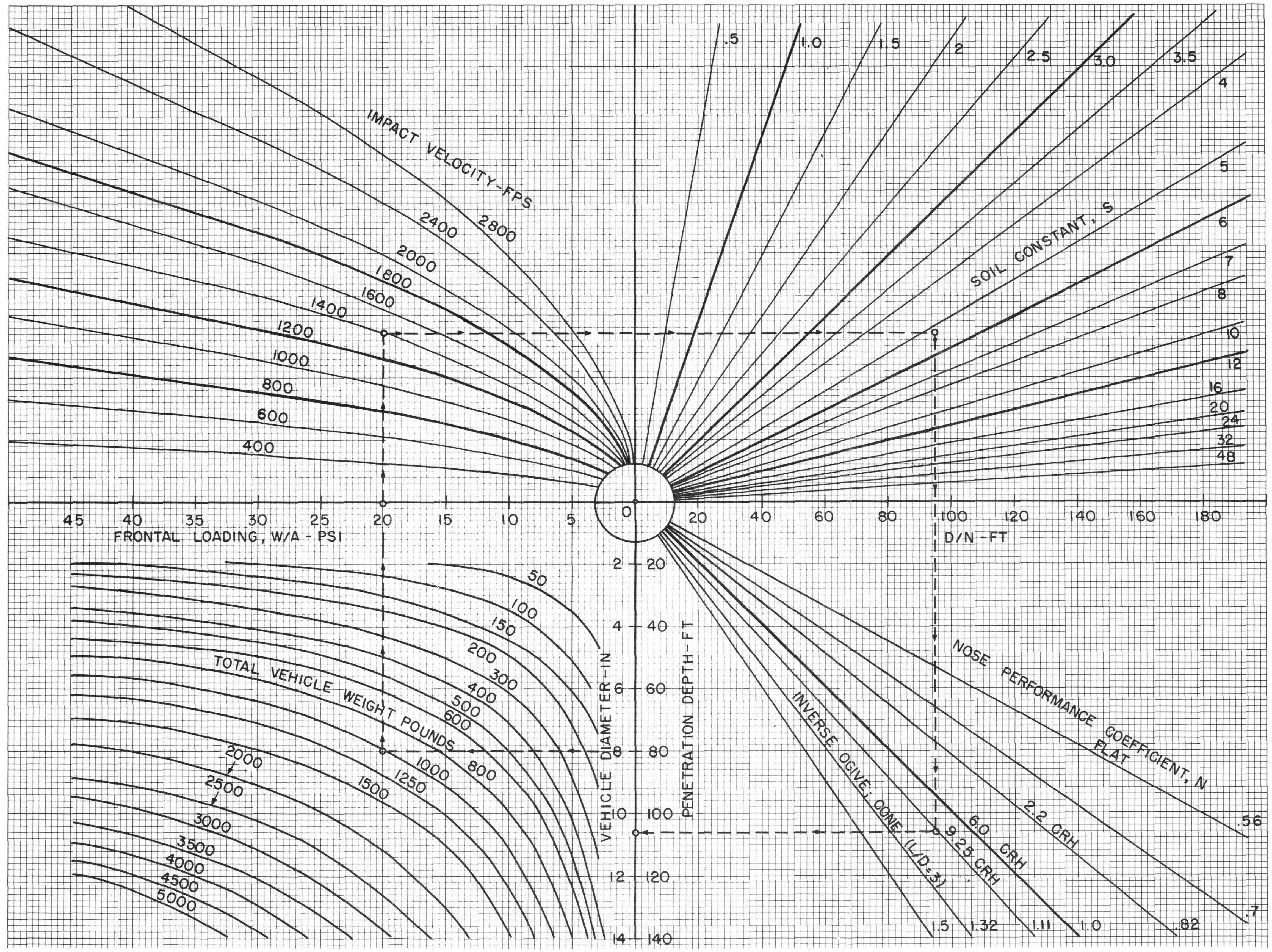

Figure 7. High-Velocity-Penetration Nomogram

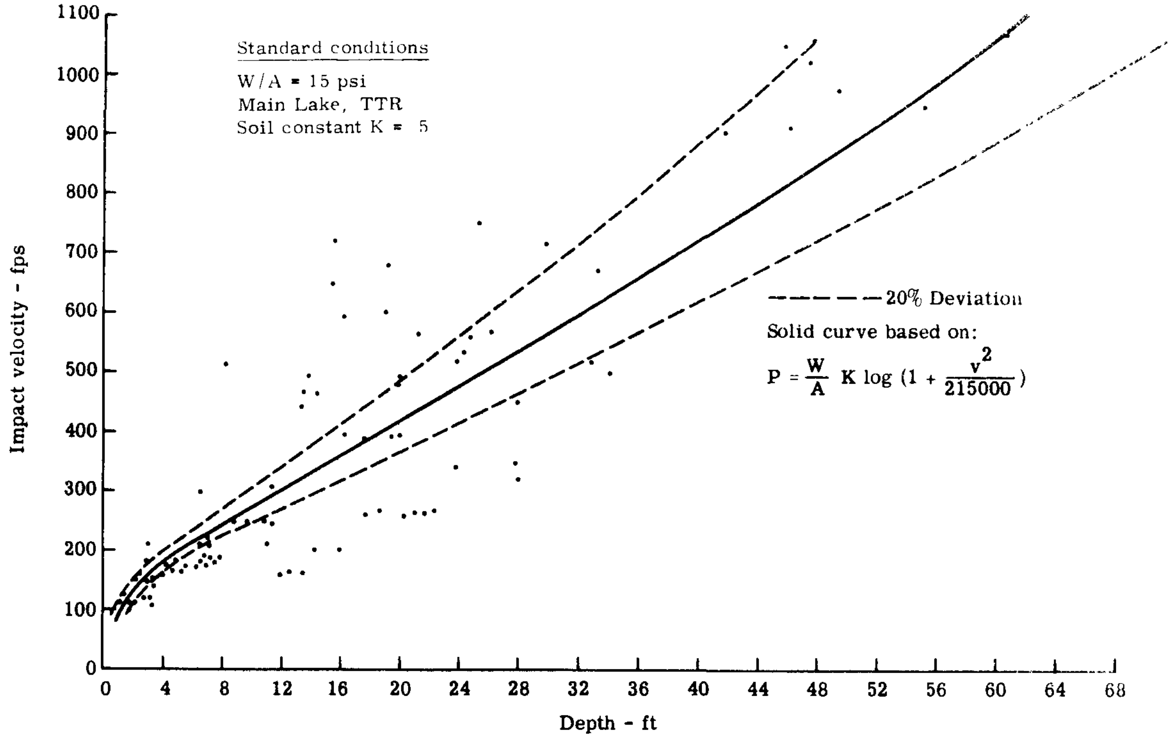

Figure 8. Data Fit to Petry Equation

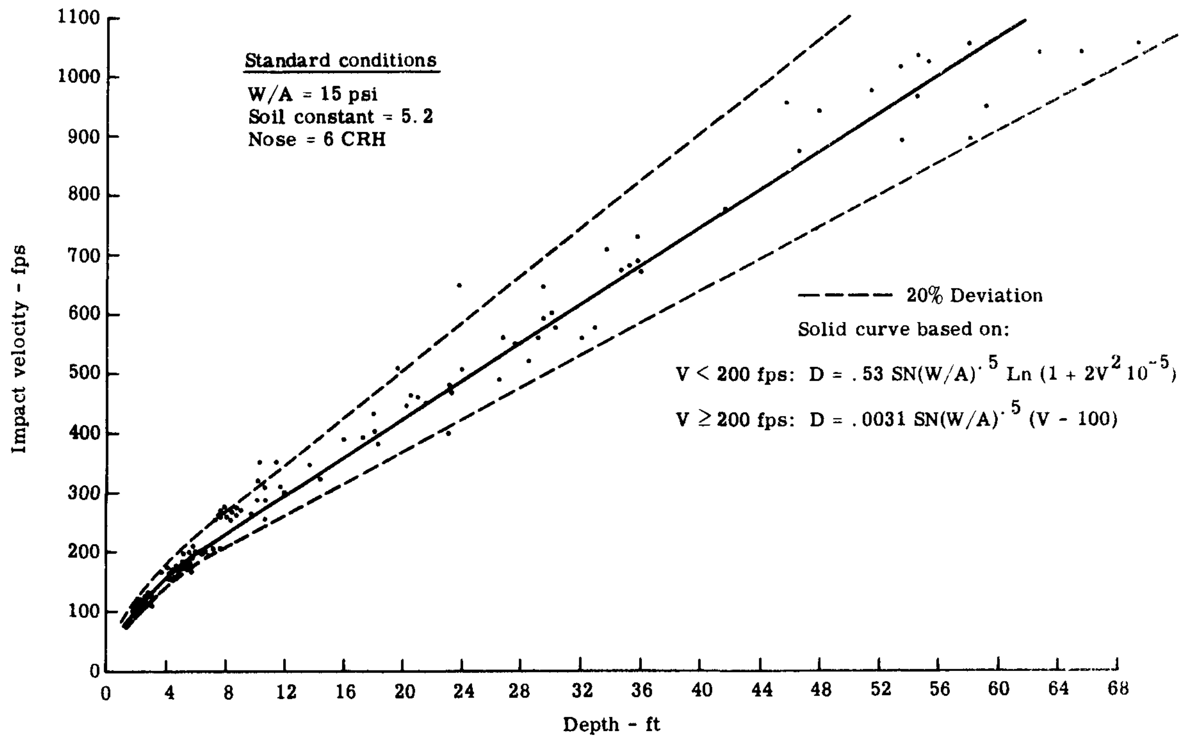

Figure 9. Final Data Fit

Conclusions

The proposed equation for the prediction of depth of earth penetration is:

$$D = 0.53SN(W/A)^{\frac{1}{2}} \ln(1 + 2V^2 10^{-5}), \qquad V < 200 \text{ feet per second}$$

$$D = 0.0031SN(W/A)^{\frac{1}{2}}(V - 100), \qquad V \geq 200 \text{ feet per second.}$$

The equation is expected to apply for all soils for which a soil constant is known or may be reasonably predicted. Also, the above equation may be used for layered media, provided the soil constant for each layer is known.

The accuracy of the proposed equation is most strongly dependent upon the accuracy with which the soil constant was determined, but for the tests considered in this analysis the deviation between the predicted and actual penetration depths exceeded 20 percent on 9 percent of the tests, and exceeded 25 percent on less than 1.5 percent of the tests.

LIST OF REFERENCES

1. Poncelet, Jean V., Cours de Méchanique Industrielle, 1829, First Edition.
2. Petry, L., Monographies de Systémes d' Artillerie, Brussels, 1910.
3. Brooks, W. B., and Reis, G. E., Soil Penetration Theory, Sandia Laboratory, SC-4950(RR), September 1963.
4. Laumbach, D. D., A Soil Penetration Analysis Applied to Experimental Data, Sandia Laboratory, SC-TM-64-57, March 1964.
5. Harri, J., Soil Penetration Theory, SCTM 225-62(71), December 1962.
6. Thompson, L. J., Dynamic Penetration of Selected Projectiles into Particulate Media, Sandia Laboratory, SC-RR-66-376, July 1966.
7. Young, C. W., and Ozanne, G. M., Low Velocity Penetration Study, Sandia Laboratory, SC-RR-66-118, July 1966.
8. Young, C. W., and Ozanne, G. M., Compilation of Low Velocity Penetration Data, Sandia Laboratory, SC-RR-66-306, June 1966.
9. Young, C. W., Low Velocity Penetration Study, Second Phase, SC-DR-66-543.
10. Young, C. W., Low Velocity Penetration Study, Wendover Operation, Sandia Laboratory, Sandia Laboratory, SC-TM-66-2611, February 1967.
11. Young, C. W., Low Velocity Penetration Tests into Natural Selenite and Gypsite, Sandia Laboratory, SC-DR-66-2695, March 1967.

APPENDIX A

DATA NORMALIZATION TECHNIQUE

It is highly impractical to attempt to obtain sufficient quantities of data at a precise set of conditions. Therefore, it is necessary to normalize the available data to a standard set of conditions so that one function or parameter may be studied at a time.

The Petry equation,

$$P = W/AK \log (1 + V^2/215,000),$$

where:

- P = depth, feet
- K = soil constant
- V = impact velocity, feet per second
- W = weight, pounds
- A = area, square inches

was used to normalize the data on the first iteration in the determination of $f_1(N)$. The Petry equation was selected because at the beginning of this analysis it was the most accurate depth prediction equation available.

An example of normalized data is Test No. 279-4, which deviates from the normal, or standard, in that the velocity is 113 feet per second, instead of 170 feet per second. Let subscripts "a" and "n" refer to "actual" and "normalized" values:

$$\frac{P_n}{P_a} = \frac{\log\left(1 + \frac{V_n^2}{215,000}\right)}{\log\left(1 + \frac{V_a^2}{215,000}\right)},$$

$$\frac{P_n}{2.0} = \frac{\log\left(1 + \frac{170^2}{215,000}\right)}{\log\left(1 + \frac{113^2}{215,000}\right)},$$

$$P_n = 2\,\frac{\log\left(1 + \frac{170^2}{215,000}\right)}{\log\left(1 + \frac{113^2}{215,000}\right)} = 4.26 \text{ ft.}$$

To minimize the error due to normalizing the data, only tests of moderate deviation from the standard were used in normalizing data.

The Petry equation was used on the first iteration of each of the functions, and then on successive iterations the more exact equation as being developed was used.

APPENDIX B

THE SOIL FUNCTION EXPRESSED IN TERMS OF SOIL PROPERTIES

To date, a lack of dynamic soil properties has prevented the development of a soil function in terms of soil properties. However, test equipment is currently being developed under contract to Sandia Laboratory which should aid in the acquisition of the necessary dynamic soil properties. The following technique, as first suggested by L. J. Thompson, Professor of Soil Mechanics, Texas A & M University, is presented to demonstrate how fundamental soil properties may be used to express soil penetrability.

$$S = f(x_1, x_2, x_3, x_4, x_5, \ldots x_i) = f(x_i),$$

where

x_1 = cohesive strength of the soil

x_2 = angle of internal friction of the soil

x_3 = apparent soil viscosity

x_4 = soil density or relative density with critical density used as reference

x_5 = degree of saturation of the soil

x_i = any other soil properties determined to be of significance.

The function of S can be expanded in a generalized Taylor's series about a point. If there are only five parameters or variables to be considered, the task becomes one of finding the equation of S in six-dimensional space. For very homogeneous materials, the average soil properties may be used to determine the average value of S. For nonhomogeneous soils, the acceleration-time trace may be used, by which the force-resisting penetration through each increment of depth may be determined, thus providing an infinity of data points for solving the general function of S.

The detailed procedure is to expand S in the generalized Taylor's series about a point "a" in the six-dimensional space to obtain the following relation, assuming that only the five soil properties given are significant:

$$f(x_1, x_2, x_3, x_4, x_5) = h(a_1, a_2, a_3, a_4, a_5) + \sum_{i=1}^{i=5}(x_i - a_i)\left(\frac{\partial f}{\partial x_i} \text{ at } a_1, a_2, a_3, a_4, a_5\right)$$

$$+ \frac{1}{2!}\sum_{i=1}^{i=5}\sum_{j=1}^{j=5}(x_i - a_i)(x_j - a_j)\left(\frac{\partial^2 f}{\partial x_i \partial x_j} \text{ at } a_1, a_2, a_3, a_4, a_5\right)$$

$$+ \frac{1}{3!}\sum_{i=1}^{i=5}\sum_{j=1}^{j=5}\sum_{k=1}^{k=5}(x_i - a_i)(x_j - a_j)(x_k - a_k)\left(\frac{\partial^3 f}{\partial x_i \partial x_j \partial x_k} \text{ at } a_1, a_2, a_3, a_4, a_5\right)$$

$$+ \ldots\ldots\ldots\ldots\ldots ,$$

where a_i is equal to the value of x_i at point a, and where $h(a_1, a_2, a_3, a_4, a_5)$ is the value of $f(x_1, x_2, x_3, x_4, x_5)$ at a. The same form of an equation can be generated for points b, c, d, etc. The partial derivatives are the constants that must be evaluated to generate the necessary function.

Enough data points must be taken to correspond to the number of unknown coefficients in the Taylor expansion and solve for these coefficients simultaneously, using a least-squares type of surface fitting procedure.

Using the available static soil properties, the above technique may provide an approximation of the soil function. As dynamic soil properties become available, the solution may be greatly improved; but for the present, and perhaps for the next few years, experimentally determined soil constants must be used.

APPENDIX C

DEPTH PREDICTION IN A LAYERED SOIL

To use Equations (8) and (9) directly, it must be assumed that the soil constant does not vary, or that an average soil constant is used. Depth of penetration into layered soils can be predicted, however, if the equations are used for each layer individually. Figure C-1 shows schematically a layered soil into which the depth of penetration may be predicted, and shows the soil vertical profile in terms of the soil constants. An example of the depth prediction technique follows.

1. Assume the soil has three layers with soil constants S_1, S_2, and S_3. The impact velocity is V_1, and is assumed to be greater than 200 fps. The first step in the analysis is to apply Equation (9) directly, using the impact velocity V_1 and soil constant S_1.

2. The depth predicted in step 1 is only a hypothetical depth, to be indicated by a primed symbol. By using the depth, D_1', it is possible to determine the velocity at D_1, which is the interface between soil S_1 and soil S_2 (see Figure C-1). The velocity V_2 is calculated as follows:

$$V_1^2 = 2a_1 D_1'$$

$$a_1 = V_1^2/2D_1'$$

$$V_1^2 - V_2^2 = 2a_1 D_1$$

$$V_2^2 = V_1^2 - 2a_1 D_1$$

$$V_2 = \sqrt{2a_1 (D_1' - D_1)} = V_1 \sqrt{1 - \frac{D_1}{D_1'}} \quad .$$

3. Depending upon whether V_2 is less or greater than 200 feet per second, Equation (8) or (9) may again be applied, using V_2 as the velocity and soil constant S_2. The depth determined by Equation (8) or (9) must be added to D_1 to give the new hypothetical depth D_2' which is then used to determine V_3:

$$V_2^2 = 2a_2 (D_2' - D_1)$$

$$a_2 = \frac{V_2^2}{2(D_2' - D_1)}$$

$$V_2^2 - V_3^2 = 2a_2 (D_2 - D_1)$$

$$V_3^2 = V_2^2 - 2a_2 (D_2 - D_1)$$

$$V_3 = \sqrt{2a_2 (D_2' - D_2)} = V_2 \sqrt{\frac{D_2' - D_2}{D_2' - D_1}} \quad .$$

4. Again, either Equation (8) or (9) may be applied, depending on whether V_3 is less than or greater than 200 feet per second, using V_3 as the impact velocity, and soil constant S_3. The depth as determined must be added to D_2 to give the final depth of penetration D_f.

Obviously this technique may be applied to any number of layers, provided the soil constant of each is known. In general, for deep penetrations through several layers, an average constant encompassing all layers is adequate. For only two or three layers of soil of radically different soil properties (such as the Salt Target at WSMR and the Main Dry Lake at TTR), the above technique provides a considerably more accurate depth prediction than that obtained by using a single average soil constant.

Test No. 279-30 will be used to demonstrate the method of depth prediction for layered soils.

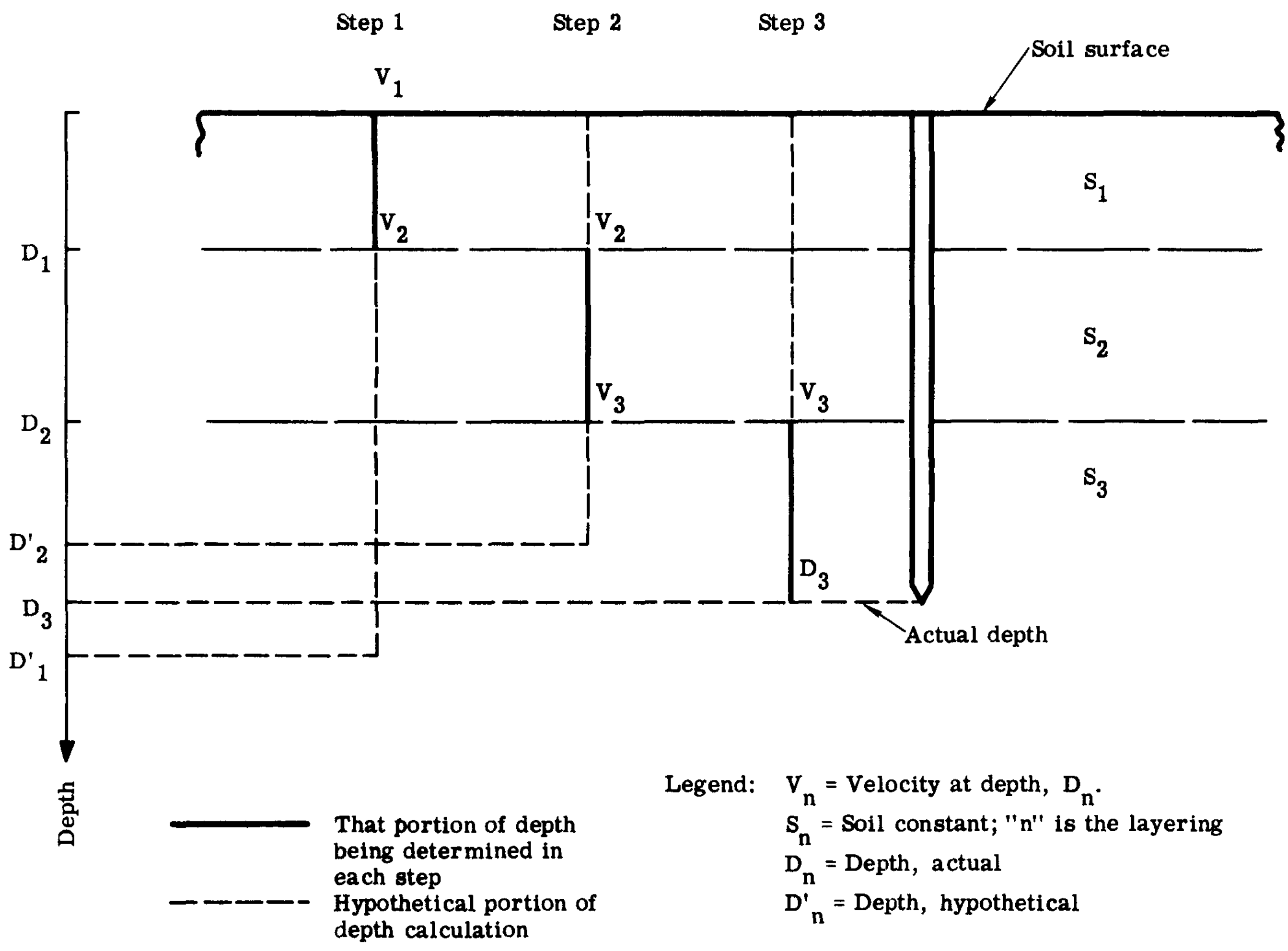

Figure C-1. Depth of Penetration Prediction for Layered Soils

For each layer, the average soil constants are 40 and 6.5 for the soft top layer and harder subsurface layer, respectively. It is also known that the top soft layer extends down to about 20 inches below grade. The vehicle and test parameters are:

$$V_1 = 173 \text{ fps}$$

$$N = 1.11 \text{ (9.25 CRH)}$$

$$W/A = 10 \text{ psi.}$$

Equation (8) may be applied to obtain D_1':

$$D_1' = 0.53SN\left(\frac{W}{A}\right)^{\frac{1}{2}} \ell n(1 + 2V^2 10^{-5})$$

$$= 0.53(40)(1.11)(10)^{\frac{1}{2}} \ell n\left(1 + 2\,[173]^2\, 10^{-5}\right)$$

$$= 35 \text{ ft.}$$

The final depth is then calculated as:

$$V_2 = V_1 \sqrt{1 - \frac{D_1}{D_1'}}$$

$$= 173 \sqrt{1 - \frac{20}{12\,(35)}}$$

$$= 168 \text{ fps}$$

$$D_f = D_1 + 0.53SN\left(\frac{W}{A}\right)^{\frac{1}{2}} \ell n(1 + 2V^2 10^{-5})$$

$$= \frac{20}{12} + 0.53\,(6.5)\,(1.11)\,(10)^{\frac{1}{2}} \ell n(1 + 2\,[168]^2\, 10^{-5})$$

$$= 1.67 + 5.4 = 7.07 \text{ ft.}$$

Measured depth = 6.4 ft.

$$\text{Deviation} = \frac{(7.07 - 6.4)}{6.4}\,(100) = 9.3\%$$

[redacted]

U. S. Atomic Energy Commission (3)
Division of Technical Information
Reports Section
Headquarters Library, G-017
Washington, D. C. 20545

Brig. General Delmar L. Crowson, USAF (2)
Director of Military Application
U. S. Atomic Energy Commission
Washington, D. C. 20545

Honorable William J. Howard (1)
Assistant to the Secretary of Defense
(Atomic Energy)
Office of the Secretary of Defense
Washington, D. C. 20301

Advanced Research Projects Agency (4)
The Pentagon, Room 3D-148
Washington, D. C. 20301

Document Control Officer (1)
Office Chief of Research and Development
Department of the Army, Room 3D-442
The Pentagon, Washington, D. C. 20310

Commanding General (2)
Army Materiel Command
Washington, D. C. 20315
Attn: AMCAD-SA-N

Headquarters, USAF (1)
AFRDC
DSC/Research and Development
Washington, D. C. 20330

Office, Chief of Engineers (1)
Department of the Army
Washington, D. C. 20315

Security Officer (1)
Office of the Assistant Chief of Staff
for Force Development
Department of the Army
Washington, 25, D. C.

Commanding Officer, Picatinny Arsenal (1)
Dover, New Jersey
Attn: Restricted Data Control Officer
For: SMUPA-TW2, Bldg. 65

Commanding General (2)
U. S. Army Munitions Command
Dover, New Jersey 07801
Attn: Restricted Data Control Officer

Commanding Officer (1)
U. S. Army Combat Developments Command
Nuclear Group
Fort Bliss, Texas 79916
Attn: Top Secret Control Officer

Commanding General (1)
U. S. Army Combat Developments Command
Fort Belvoir, Virginia 22060
Attn: Top Secret Control Officer

Commanding Officer (1)
U. S. Army Materiel Command
Field Office
Sandia Base, Albuquerque, New Mexico 87115

Los Alamos Scientific Laboratory (1)
P. O. Box 1663
Los Alamos, New Mexico 87544
Attn: W-DO

Headquarters (4)
Field Command/Defense Atomic Support Agency
Sandia Base, Albuquerque, New Mexico 87115
Attn: Adjutant General
For: Liaison Office, USACDCNG
For: FCDV-2, E & C Branch
For: AMC/FO, Sandia Base
For: Frankford Arsenal, Philadephia, Penna.

Director (2)
Air Force Weapons Laboratory (AFWL)
Attn: WLIL
Kirtland Air Force Base, New Mexico 87117
For: WLAW-3
For: Headquarters, USAF, AFRDPF

University of California (5)
Lawrence Radiation Laboratory
P. O. Box 808
Livermore, California 94551
Attn: Technical Information Division

U. S. Atomic Energy Commission (1)
Albuquerque Operations Office
P. O. Box 5400
Albuquerque, New Mexico 87115

U. S. Atomic Energy Commission (1)
Sandia Area Office
P. O. Box 5400
Albuquerque, New Mexico 87115

Atomics International (2)
P. O. Box 309
Canoga Park, California 91304

Battelle Memorial Institute (1)
505 King Avenue
Columbus, Ohio 43201

General Electric Company (1)
Valley Forge Space Technology Center
P. O. Box 8555
Philadelphia, Pennsylvania 19101
Attn: Space Sciences Laboratory

~~SPECIFIED DISTRIBUTION ONLY~~ (Continued)

Hittman Associates, Inc. (1)
P. O. Box 2685
4715 East Wabash Avenue
Baltimore, Maryland, 21215

Lockheed Missiles and Space Company (1)
P. O. Box 504
Sunnyvale, California 94088
Attn: Nuclear Power Development

Douglas Aircraft Company, Inc. (1)
Missile and Space Systems Division
3000 Ocean Park Boulevard
Santa Monica, California 90405
Attn: Advanced Space Technology

General Atomic Division (1)
General Dynamics Corporation
P. O. Box 608
San Diego, California 92112
Attn: Library

NUS Corporation (1)
Environmental Safeguards Division
Suite 1100
1730 M Street, N. W.
Washington, D. C. 20036
Attn: M. S. Goldman, Vice President

Director, USAF Project RAND (1)
via Air Force Liaison Office
The Rand Corporation
1700 Main Street
Santa Monica, California 90406
Attn: Library

TRW Systems (1)
P. O. Box 287
Redondo Beach, California 90277

Westinghouse Electric Company (1)
Astronuclear Laboratory
P. O. Box 10864
Pittsburgh 30, Pennsylvania
Attn: Flight Safety Analysis Group

Texas Agricultural and Mechanical University (1)
College of Engineering
College Station, Texas 77843
Attn: Dr. L. J. Thompson

Woodward-Clyde-Sherard & Associates (1)
2811 Adeline Street
Oakland, California 94608
Attn: R. L. McNeill

W. J. Howard, 1000
W. A. Gardner, 1500
D. M. Olson, 1510
B. E. Arthur, Jr., 1520
T. B. Lane, 1540
R. W. Henderson, 2000
W. Van Deusen, 3114
R. C. Fletcher, 5000
T. B. Cook, 5200
B. F. Murphey, 5230
J. W. Weihe, 5250
L. D. Smith, 5500
A. A. Lieber, 5540
D. B. Shuster, 5600
F. W. Neilson, 5620
R. G. Clem, 5630
W. F. Roherty, 5633
L. E. Hollingsworth, 7200
T. L. Pace, 7210
R. S. Millican, 7212
R. D. Robinett, 7215
R. L. Brin, 7220
G. L. Miller, 7223
B. S. Biggs, 8000
J. H. Scott, 9200
J. C. Eckhart, 9220
E. L. Harley, 9225
H. H. Patterson, 9230
J. E. Hinde, 9231
A. E. Bentz, 9232
A. Y. Pope, 9300
V. E. Blake, Jr., 9310
R. C. Maydew, 9320
H. R. Vaughn, 9321
W. H. Curry, 9322
E. C. Rightley, 9323
W. R. Barton, 9324
J. K. Cole, 9325
K. J. Touryan, 9326
W. N. Caudle, 9327 (15)
A. J. Clark, 9330
B. F. Hefley, 8232
B. R. Allen, 3421
W. K. Cox, 3428-1
W. F. Carstens, 3410
Attn: R. S. Gillespie, For: DTIE (3)
For: H. F. Carroll (1) For: W. H. Swiss (1)